

# Comparison Study of Input Shaping Techniques to Control an Underactuated Flexible Link System

*Yasser Al Hamidi\* and Micky Rakotondrabe*

*University of Franche-Comté*

*FEMTO-ST Institute, CNRS / UBFC / UFC / ENSMM / UTBM*

*24, rue Alain Savary*

*25000 Besançon France*

*\*corresponding author: yasser.al-hamidi@qatar.tamu.edu*

## **ABSTRACT**

This paper compares between three different input shaping feedforward techniques, traditional (TIS), extra insensitive (EI), and modified input shaping (MIS), to reduce the vibration of a flexible link QUANSER system. The main challenge is that the system under test is an underactuated system: it has one input and two outputs. This makes the application of the input shaping techniques not utilizable directly. We therefore first propose to use a variable change at the output in order to make the process equivalent to a monovariate system without modification of the behavior and of the objective of the control. The experimental tests demonstrate the efficiency of the technique and the different results from the three control techniques are compared and discussed. It comes out that EI shapers are the most efficient in term of robustness. MIS shaper has a shorter length than that of a corresponding TIS shaper; however both shapers have the same ability of vibration suppression. Also MIS scheme is easier than the traditional scheme because the numerical optimization is unnecessary in the design of the MIS shaper. MIS shaper has an advantage over a TIS corresponding shaper in being capable of suppressing multimode of vibration

## **INTRODUCTION**

Vibration is a significant problem in dynamical systems that require performing precise motion in presence of structural flexibility. The performance of precision motion depends on damping capacity of the system which can be enhanced by passive or active damping methods. In the passive method, damping is increased by deploying external dampers such as viscous dampers. Feedback and Feedforward control techniques can also be used as an active approach in a wide range of applications. In this paper we will propose to reduce by feedforward control the residual vibration of a QUANSER flexible link system. Additionally to the high oscillation of the system, a main challenge to open-loop its control is the fact that it is underactuated. The main advantage of feedforward control of vibration (oscillation) is the non-necessity of sensors, and therefore the low cost and the high packageability that are yielded. Such gains are essential in many applications where the spaces available to put convenient sensors are limited.

Various methods for controlling the vibration of flexible structures have been studied and can be roughly divided into feedback and feedforward methods. While feedback control schemes have been demonstrated to effectively reduce vibration, the performance of feedback techniques can often be improved by additionally using feedforward controllers that alter the actuator commands in order to achieve vibration reduction. One feedforward approach, known as input shaping, has

been successfully applied for controlling flexible structures and reduce their residual vibration. The first self-canceling command generation was developed in the 1950's by O.J.M. Smith [1]. Called posicast control, this method involved breaking a command of a certain magnitude into two smaller magnitude commands, one of which is delayed one-half period of vibration. Unfortunately, this technique was not robust to modeling uncertainties [2]. Singer and Seering developed reference commands that were robust enough to be effective on a wide range of systems [3]. This new robust technique is named as input shaping. Input shaping is implemented by convolving a sequence of impulses, with a desired system command to produce a shaped input [4]. Input shaper is designed by generating a set of constraint equations which limit the residual vibration, maintain actuator limitations, and ensure some level of robustness to modeling errors. By solving the set of constraints, the amplitudes and time locations of the impulses are determined [5]. If the constraints are minimum duration and zero residual vibration, then the solution shaper is ZV (zero vibration) shaper. However, ZV shaper is not well on most systems because it is sensitive to modeling errors. Robustness can be improved by adding more impulse to the shaper. The resulting shaper is a three step (TS) shaper. Direct solution of amplitudes and their duration is not possible due to the inadequate number of constraint equations. ZVD (zero vibration derivative) shaper, as a special solution, can be obtained by setting the derivation of constraint equations with respect to the frequency of the residual vibration equal to zero. ZVD scheme is less sensitive to timing error; however, it requires a time penalty. ZVD shaper has duration of one period of unshaped vibration, while ZV has only a half period [6, 7]. To improve robustness to modeling errors Tuttle and Searing (1994) developed a zero placement method to design multi-mode input shapers by placing zeros near the system poles [8]. In 1999 Singhose and Mills used acceptable residual vibration to obtain more robust control results, and called this method the Extra Insensitive (EI) shaper [9]. Park et al. (2001) proposed a graphical approach to design robust multi-hump EI shaper in the z-plane [10]. Shan in 2005 proposed a modified input shaping (MIS) method which get a better performance, shorter length, and have the same ability of vibration suppression like other shapers [11].

These aforementioned works deal with the control of one axis flexible systems, i.e. monovariable systems. They cannot therefore be applied to multi-axis flexible system which is the case of the QUANSER flexible link treated in this paper. The system is composed of two output axis where one of which only is actuated (one input, two outputs), and therefore underactuated. Both the two axis exhibit badly damped oscillation. In this paper, by combining the two outputs into one absolute output, a model that is utilized to design the input shaping compensators is yielded. Three input shaping techniques are explored, designed and the flexible link: the analyzed: the zero vibration techniques (ZV) which include particularly the three steps input shaping technique (TS), the extra-sensitive technique (ES) and the modified technique (MIS). The different results are compared in term of capability of damp both the two oscillations and in term of robustness face to parameters uncertainties.

The remainder of this paper is organized as follows. In section-2, we review the three input shaping techniques. Section-3 is devoted to the experimental tests and results. In section-4, we give the comparisons and the discussions about the performances of the three techniques. Finally, we end the paper by some conclusions in section-5.

## THEORETICAL BACKGROUND

Consider a second order system

$$G(s) = \frac{y(s)}{u(s)} = \frac{G_o}{\frac{1}{(\omega_n)^2} s^2 + 2 \frac{\zeta}{\omega_n} s + 1}$$

Where  $y$  is the output,  $u$  is the driving input,  $\omega_n$  is the natural frequency,  $\zeta$  is the damping ratio and  $G_o$  is the static gain. To feedforward control this system, a compensator based on an input technique can be used (Figure1). This compensator is also called shaper in this case. In the figure,  $y_r$  is the reference input.

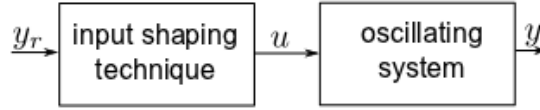


**Figure 1: Block diagram of a feedforward control of oscillation by an input shaping technique**

The main idea of input shaping techniques revolves around applying a series of impulses as a command  $u$  to the system such that the different oscillating impulse responses thwart themselves, the response of the  $i$ -th impulse of amplitude  $A_i$  and applied at time  $t_i$  being:

$$y_i(t) = G_o A_i \frac{\omega_n}{\sqrt{1-\zeta^2}} e^{-\zeta \omega_n (t-t_i)} \sin\left(\omega_n \sqrt{1-\zeta^2} (t-t_i)\right)$$

One important measure to characterize the damping efficiency is the residual amplitude. The residual vibration amplitude is obtained at the time of the last impulse,  $t_n$  as

$$V(\zeta, \omega) = e^{-\zeta \omega_n t_n} \sqrt{C^2(\zeta, \omega) + S^2(\zeta, \omega)} \quad (1)$$

$$C(\zeta, \omega) = \sum_{j=1}^n A_j e^{\zeta \omega_n t_j} \cos(\omega_d t_j) \quad (2)$$

Where

$$S(\zeta, \omega) = \sum_{j=1}^n A_j e^{\zeta \omega_n t_j} \sin(\omega_d t_j) \quad (3)$$

The shaper, i.e. the compensator, is based on the impulses. Hence, for any input reference  $y_r$ , the driving command  $u$  is a convolution between these impulses and  $y_r$ . Each input shaping technique possesses its proper method to calculate the amplitude  $A_i$  and its application time  $t_i$  which are based on some constraints.

For traditional input shaping, i.e. the ZV technique, Eq. (2) and Eq. (3) should be independently equal to zero to achieve vibration free response after the last impulse [12]. Amplitudes and time locations of the ZV shaper is shown in Eq. (4) as first and second rows respectively.

$$ZV = \begin{bmatrix} \frac{1}{1+K} & \frac{K}{1+K} \\ 0 & \frac{\pi}{\omega_d} \end{bmatrix} \quad \text{where} \quad K = e^{\frac{-\zeta\pi}{\sqrt{1-\zeta^2}}} \quad (4)$$

An impulse addition to ZV produces Three Step (TS) shaper. A specific analytical solution can be obtained by making the derivative of the constraint equations (2) and (3) with respect to natural frequency of the system equal to zero,  $dC/d\omega_n = 0$  and  $dS/d\omega_n = 0$ . The resulting shaper is called Zero Vibration and Derivative, ZVD. Amplitudes and time locations of the ZVD shaper is shown in Eq. (5) as first and second rows respectively.

$$ZVD = \begin{bmatrix} \frac{1}{1+2K+K^2} & \frac{2K}{1+2K+K^2} & \frac{K^2}{1+2K+K^2} \\ 0 & \frac{\pi}{\omega_d} & \frac{2\pi}{\omega_d} \end{bmatrix} \quad (5)$$

The next two derivative-method shapers, the zero vibration and double derivative (ZVDD) and zero vibration and triple derivative (ZVDDD), are described by:

$$ZVDD = \begin{bmatrix} \frac{1}{1+3K+3K^2+K^3} & \frac{3K}{1+3K+3K^2+K^3} & \frac{3K^2}{1+3K+3K^2+K^3} & \frac{K^3}{1+3K+3K^2+K^3} \\ 0 & \frac{\pi}{\omega_d} & \frac{2\pi}{\omega_d} & \frac{3\pi}{\omega_d} \end{bmatrix} \quad (6)$$

$$ZVDDD = \begin{bmatrix} \frac{1}{D} & \frac{4K}{D} & \frac{6K^2}{D} & \frac{4K^3}{D} & \frac{K^4}{D} \\ 0 & \frac{\pi}{\omega_d} & \frac{2\pi}{\omega_d} & \frac{3\pi}{\omega_d} & \frac{4\pi}{\omega_d} \end{bmatrix} \quad (7)$$

Where  $D = 1 + 4K + 6K^2 + 4K^3 + K^4$

Extra Insensitive (EI) input shapers are designed to allow a nonzero value  $V$  residual vibration. Extra Insensitive input shapers have the same impulse locations as the TIS ZVD shapers but have different impulse amplitude values that lead to greater robustness [14]. For this type of shapers residual vibration remains below some tolerable level,  $V_{tol}$ , at the modeled frequency. For a system

with viscous damping, the EI shaper is described by:

$$EI = \begin{bmatrix} A_1 & 1-(A_1+A_3) & A_3 \\ 0 & t_2 & T_d \end{bmatrix} \quad (8)$$

Where  $A_1 = 0.24968 + 0.24962V_{tol} + 0.80008V_{tol}\zeta + 0.49599\zeta^2 + 3.17316V_{tol}\zeta^2$

$$A_3 = 0.25149 + 0.21474V_{tol} - 0.83249\zeta + 1.41498V_{tol}\zeta + 0.85181\zeta^2 - 4.9009V_{tol}\zeta^2$$

$$t_2 = T_d \left( \begin{array}{l} 0.49990 + 0.46159V_{tol}\zeta + 1.75601V_{tol}\zeta^3 + \\ 8.57843V_{tol}^2\zeta - 108.644V_{tol}^2\zeta^2 + 36.989V_{tol}^2\zeta^2 \end{array} \right)$$

Shapers that extend this idea have a progressively larger number of humps and are called multi-hump EI shapers [15].

The modified input-shaping (MIS) technique simplifies the shaper design by eliminating the need to use numerical optimization [11]. This technique forms MISZV (modified input shaping zero vibration) shapers that have zero vibration at the modeled frequency, but have a larger number of impulses and longer shaper duration than the ZV shaper. An  $n$ -impulse MISZV shaper is described by:

$$N\text{-impulse MISZV} = \begin{bmatrix} \frac{1}{1+M} & \frac{K}{1+M} & \dots & \frac{K^{i-1}}{1+M} & \frac{K^{n-1}}{1+M} \\ 0 & \frac{T_d}{n} & \dots & \frac{(i-1)T_d}{n} & \frac{(n-1)T_d}{n} \end{bmatrix} \quad (9)$$

Where  $M = K + \dots + K^{i-1} + K^{n-1}$  and  $K = e^{-2\zeta\pi/n\sqrt{1-\zeta^2}}$

The length of the N-impulse shaper is  $(N-1)T_d/N$ ; which increases with the increase of  $N$ ; and the minimal value is  $T_d/2$  if  $N=2$  ( $T_d$  is the uncompensated residual vibration period). MIS shapers are identified by impulse number and a distinguishable character MIS, i.e. 2-, 3-impulse MIS ZV shaper, etc. Here, the character MIS is added to distinguish the shapers obtained by using the MIS technique from those shapers developed by other methods. In this type of shapers, the improvement in robustness to system parameter variations can be realized by convolving two MISZV shapers designed for the same frequency [11]. The resulting MISZVD shaper is indicated by the number of impulses of each of the MISZV shapers used to create it. An  $N \times M$ -impulse MISZVD is formed by convolving an MISZV shaper containing  $N$  impulses with an MISZV shaper with  $M$  impulses. Convolving MISZV shapers of higher number of impulses results in more robust MISZVD

shapers, at the cost of increased shaper duration. It should be noted that a 2x2-impulse MISZVD shaper is the traditional ZVD shaper. A 2 x3 – impulse MISZVD has the following expression:

$$2\_3\text{-impulseMISZVD} = \begin{bmatrix} \frac{1}{1+M} & \frac{K^2}{1+M} & \frac{K^3}{1+M} & \frac{K^4}{1+M} & \frac{K^5}{1+M} & \frac{K^7}{1+M} \\ 0 & \frac{T_d}{3} & \frac{T_d}{2} & \frac{2T_d}{3} & \frac{5T_d}{6} & \frac{7T_d}{6} \end{bmatrix} \quad (10)$$

Where  $M=K^2+K^3+K^4+K^5+K^7$  and  $K=e^{-\zeta\pi/3\sqrt{1-\zeta^2}}$

## EXPERIMENTAL SETUP AND RESULTS

### *I. Presentation of the experimental setup*

The setup comprises of the QUANSER flexible link system to be controlled (Figure 2), and the USB Q8 QUANSER board to implement shaper (compensator) and acquire the input and output signals. The QUANSER flexible link system uses a DC motor to rotate the flexible link from one end in the horizontal plane. A quadrature encoder is mounted to the motor shaft to measure the angular position  $\theta$  of the shaft when it rotates. The flexible link, which is the bar, is instrumented with the strain gage to detect its angular deflection denoted  $\alpha$ . The final output angle relative to an absolute reference is  $\theta + \alpha$ . The encoder and the strain gauge are only used to identify the model and to validate the open-loop control technique in this paper. For the purpose of this research it is sufficient to use a simplified model that can adequately describe the motion of the end-point. This simplified model is depicted in Figure 3 as a spring attached to a plate at each end.



Figure 2: Flexible Link System

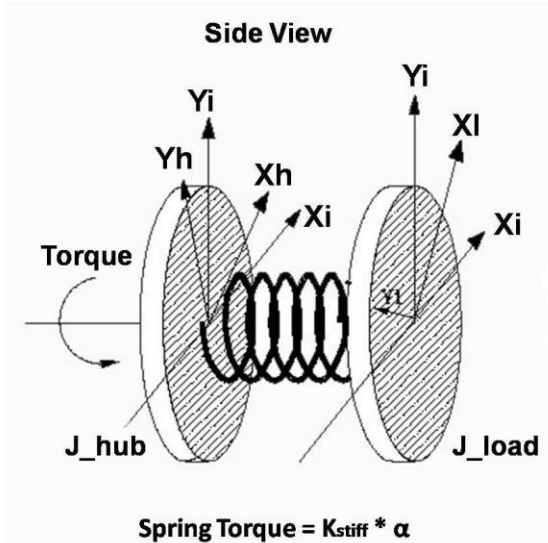


Figure 3: Simplified Model

## II. Model of the flexible link

The simplified model state space matrices are:

$$A = \begin{pmatrix} 0 & 0 & 1 & 0 \\ 0 & 0 & 0 & 1 \\ 0 & \frac{K_{stiff}}{J_{eq}} & \frac{-\eta_m \eta_g K_t K_m K_g^2 + B_{eq} R_m}{J_{eq} R_m} & 0 \\ 0 & \frac{-K_{stiff} (J_{eq} + J_{link})}{J_{eq} J_{link}} & \frac{\eta_m \eta_g K_t K_m K_g^2 + B_{eq} R_m}{J_{eq} R_m} & 0 \end{pmatrix} \quad B = \begin{pmatrix} 0 \\ 0 \\ \frac{\eta_m \eta_g K_t K_g}{J_{eq} R_m} \\ \frac{-\eta_m \eta_g K_t K_g}{J_{eq} R_m} \end{pmatrix}$$

(11)

Where  $B_{eq}$  is the equivalent viscous damping,  $\eta_m$  and  $\eta_g$  denote the motor and gearbox efficiencies respectively,  $K_t$  denotes the motor torque constant,  $K_g$  is the motor gear ratio and  $K_m$  is the back emf constant.  $V_m$  and  $R_m$  denote the motor input voltage and armature resistance respectively.

## III. Experimental results for the three feedforward control techniques

From the model of the whole flexible link, and by using the formulas in Section-2, we calculated three shapers: a shaper based on the TIS, a shaper based on the EI and a shaper based on the MIS. Each of them was implemented and applied to the QUANSER flexible link. To simulate modeling error, the modeled uncompensated vibration period  $T_p$  was deviated by different values from the actual compensated vibration period  $T_d$  for each type of the compensators.

### A. Results with the TIS technique

For the TIS, different TIS shapers of different number of impulses have been calculated and implemented: ZV (2 impulses), ZVD (3), ZVDD (4), ZVDDD (5) and ZVDDDD (6). Figure 4 depicts the resulting responses  $\theta + \alpha$ . The same figure also depicts the response without control. We can observe that ZVD TIS input shaper gives the best response without compromising the settling time which is equal to 0.7 second in this case.

### B. Results with the EI technique

The experimental responses to the 5% and 20% EI shapers are shown figures 5 and 6 respectively. The percentage in this context (Vtol %) refers to the allowable residual vibration tolerance. The responses in these two figures are shown when the shaper is designed assuming different uncertainties in the modeled natural frequency. One can see the close-to-zero vibration when the shaper is designed with a modeled frequency close the system actual natural frequency. Figure 6 also shows that the controller robustness improves when Vtol increases. This improvement in the robustness is very clear when the modeled period  $T_p$  deviated from

0.7 sec. comparing the responses for  $T_p = 0.5\text{sec}$  in both figures 5 and 6 shows that the 20% shaper performs better than the 5% shaper.

### C. Results with the MIS technique

Figure 7 shows the MIS ZV experimental responses to 2 through 6-impulses MIS ZV shapers for two different  $T_p$  values,  $T_p = 0.79\text{sec}$  which corresponds to the modeled natural frequency, and  $T_p = 0.5\text{sec}$  which deviate considerably from the modeled one. The settling time improves greatly as the modeled natural frequency gets closer to the actual one. Figure 7 below also shows that increasing the number of impulses doesn't have a great impact on the performance of the shaper.

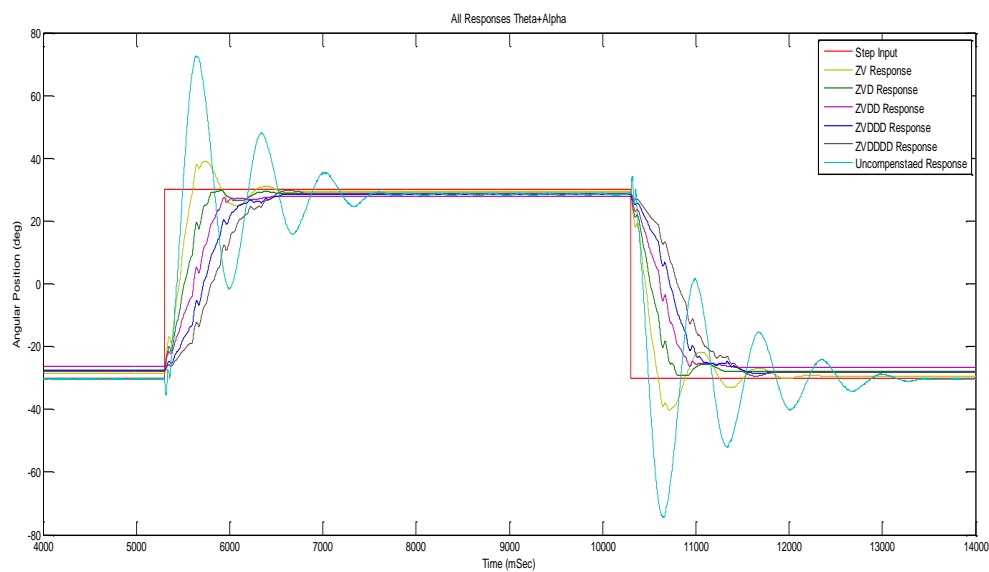


Figure 4: Tip Responses – TIS Experimental

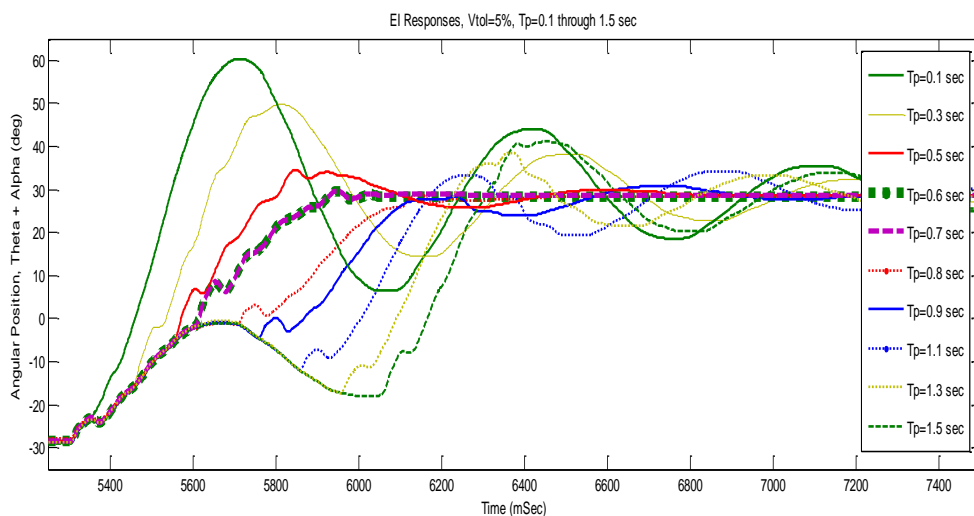
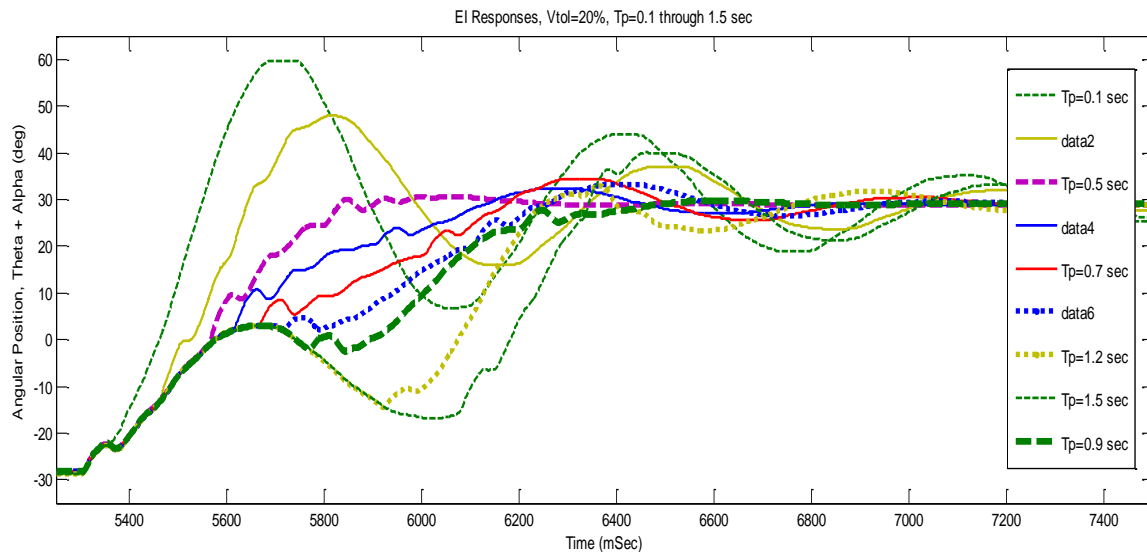
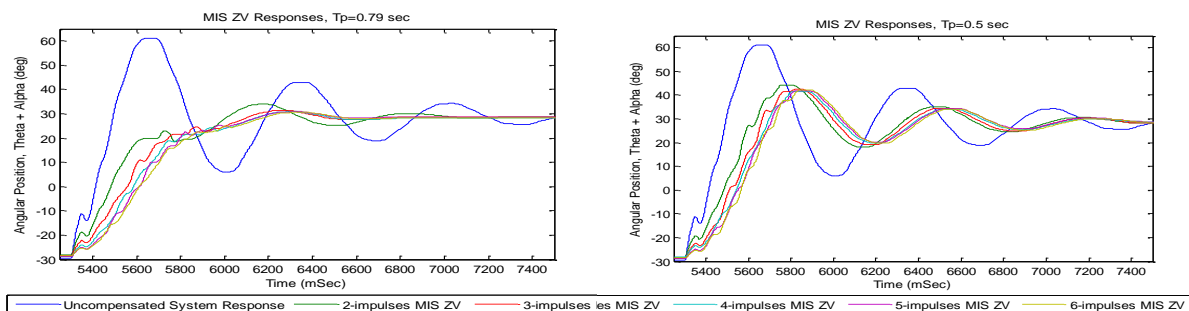


Figure 5: Actual Res. to 5% EI – Experimental





**Figure 6: Actual Res. to 20% EI – Experimental**



**Figure 7: MIS ZV Responses – Experimental**

**COMPARISON AND DISCUSSION:**

The previous experimental results and the robustness of the input shaping techniques used are discussed in this section. Sensitivity curves are used to visualize and measure the extent to which shapers are insensitive. The sensitivity curve for a TIS ZV shaper is shown by the solid blue line in Figure 8. This is obtained by putting as the vertical axis the residual vibration and as the horizontal axis the actual natural frequency, normalized relative to the identified frequency. On the other hand, insensitivity is a measure of robustness which we derive from sensitivity curve by measuring its width at a tolerable vibration level, *Vtol*. Figure 8 also shows the additional insensitivity gained from each higher-order derivative of the shaper, and it shows also that the derivative constraint flattens the sensitivity curve at the modeled frequency which in turn increases the insensitivity.

EI shapers have a sensitivity curves as pictured in figure 9. These shapers have the same impulse times as the ZVD shapers but have different amplitude values that lead to greater robustness. As *Vtol* (the dashed red line in the figure below) increases the robustness of the shaper increases as well. This is shown clearly in figures 5 and 6 in the previous EI experimental results section.

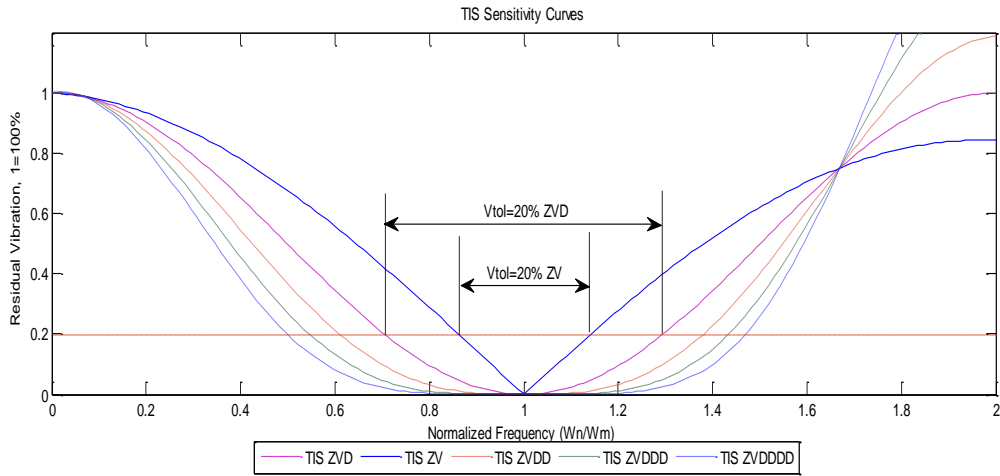


**Figure 8: TIS Sensitivity Curves – Simulation**

Figure 10 shows the frequencies at which the designed shaper gives almost zero vibration for different tolerances. The difference between the two frequencies that give zero vibration increases when  $Vtol$  increases.

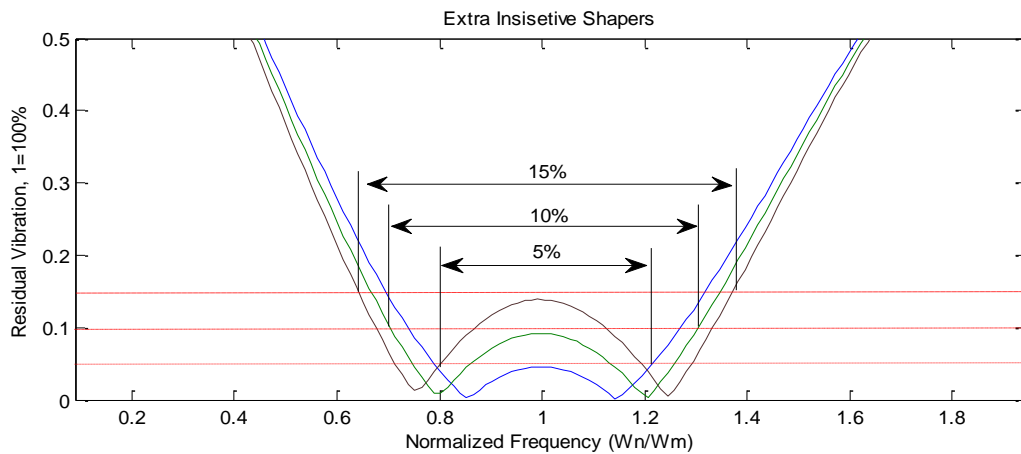


**Figure 9: EI shapers sensitivity curves - Simulation**

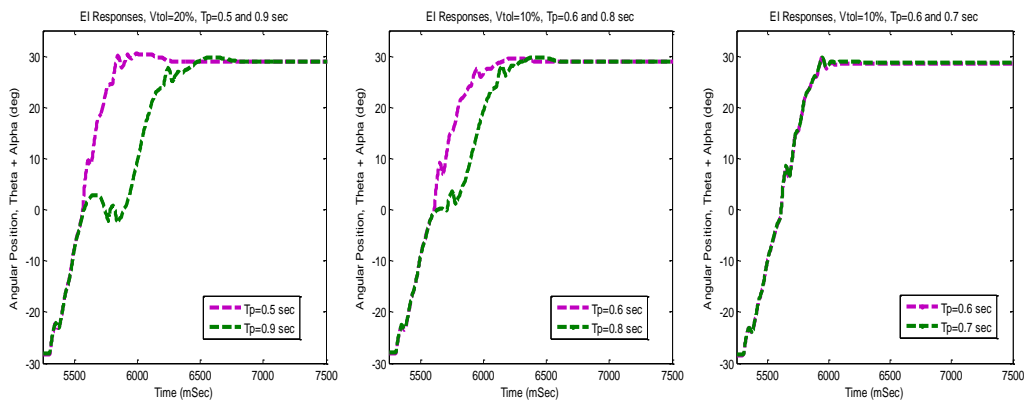


**Figure 10: EI shapers Robustness (20% for the most left, 5% for the most right) - Experimental**

The sensitivity plots for 2-impulse through 6 impulse modified TIS ZV input shapers are show in figure 11. One can see that the additional impulses only provide a minimal increase in shaper insensitivity about the modeled frequency.

Figures 12 and 13 below show the experimental  $\theta + \alpha$  responses to 3-impulse MIS ZV and 6-impulse MIS ZV input shapers respectively. Each of these figures shows the responses for 15 different frequencies having pseudo-period varying from  $T_p = 0.1\text{sec}$  through  $T_p = 1.5\text{sec}$ . One can notice that the best response occurs at  $T_p = 0.7\text{sec}$  for all MIS ZV shapers which is very close to the modeled frequency  $T_p = 0.79\text{sec}$ .

However if we zoom out a bit to see the MIS ZV sensitivity curves over a wider range of frequencies, it can be seen from figure 14 that MIS ZV shapers can suppress not only one mode of vibration with frequency ratio 1 but also infinite vibration modes with specified frequencies which vary depending on the number of impulses.

Similar to traditional input shapers, increasing the degree of robustness in modified shapers flattens the sensitivity curves about the modeled frequency, however increasing the number of impulses for the MIS ZVD shapers only provides a minimal increase in shaper insensitivity like MIS ZV shapers. Shapers with higher robustness can be obtained by convolving multiple shapers with lower robustness; and an arbitrary number of shapers can be convolved to form a new shaper with expected robustness and characteristics. For example, the convolution of a 2-impulse MIS ZV shaper with a 2x3-impulse MIS ZVD shaper can result in a 2x2x3-impulse MIS ZVDD shaper; the convolution of a 2x2-impulse MIS ZVD shaper with a 2x3-impulse MIS ZVD shaper can result in a more robust 2x2x2x3-impulse MIS ZVDDD shaper, etc. [11]. Figure 15 shows a sensitivity comparison of different shapers. And figure 16 shows the experimental responses of the same shapers.

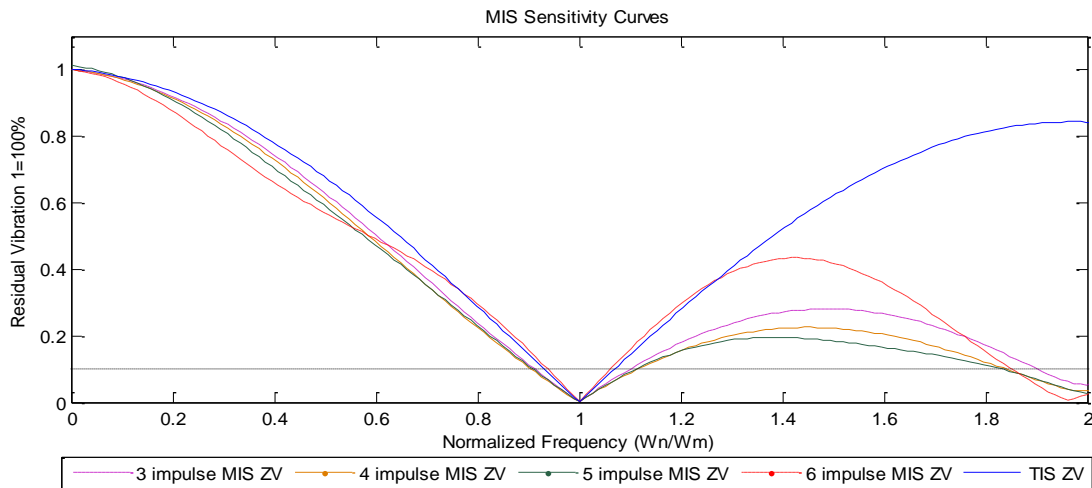


**Figure 11: MIS ZV shapers sensitivity curves – Simulation**

In summary, the zero derivative constraint flattens the sensitivity curve at the modeled frequency and increases the insensitivity. To further increase insensitivity, this process can be repeated by taking additional, higher-order derivatives. The price for each additional derivative, however, is an increase in shaper duration; note that the duration of TIS ZVD shaper is twice that of the TIS ZV

shaper. The EI shaper has the same impulse times as the TIS ZVD shaper but has different amplitude values that lead to greater robustness. The two-hump EI shaper has the same duration as the TIS ZVDD, and the three-hump EI and TIS ZVDDD have the same durations [11, 15].

The input shaping techniques presented and compared in this paper have several potential applications. Among them, piezoelectric cantilevered actuators (piezoactuators) are demonstrated to present a high Q-factor [17-18]. Input shaping techniques have been successfully developed to control single degree of freedom piezoactuators [19-20] as well as two degrees of freedom piezoactuators [21-22]. Relative to feedforward H-inf techniques [23], input shaping techniques have been shown to maintain or almost maintain the high bandwidth of these actuators.

**CONCLUSION:**

Input shaping is an effective vibration control method that has been widely studied in recent years. Three input shaping methods have been explored in this paper to control a QUANSER flexible link that is underactuated (one input, two outputs). The two outputs have been assembled into one absolute output in order to provide the model utilized to synthesize the shapers of the input shaping techniques.

The experimental results of each of the three explored shaping methods showed that, increased robustness comes at the expense of increased shaper duration and, as a result, slower system rise time. However, different shaper design methods provide robustness with different insensitivity efficiency.

Using this measure, EI shapers are the most efficient when it comes to robustness against modeling errors and parameter uncertainty. MIS shaper has a shorter length than that of a corresponding TIS shaper; however both shapers have the same ability of vibration suppression. Also MIS scheme is easier than the traditional scheme because the numerical optimization is unnecessary in the design of the MIS shaper. MIS shaper has an advantage over a TIS corresponding shaper in being capable of suppressing multimode of vibration.

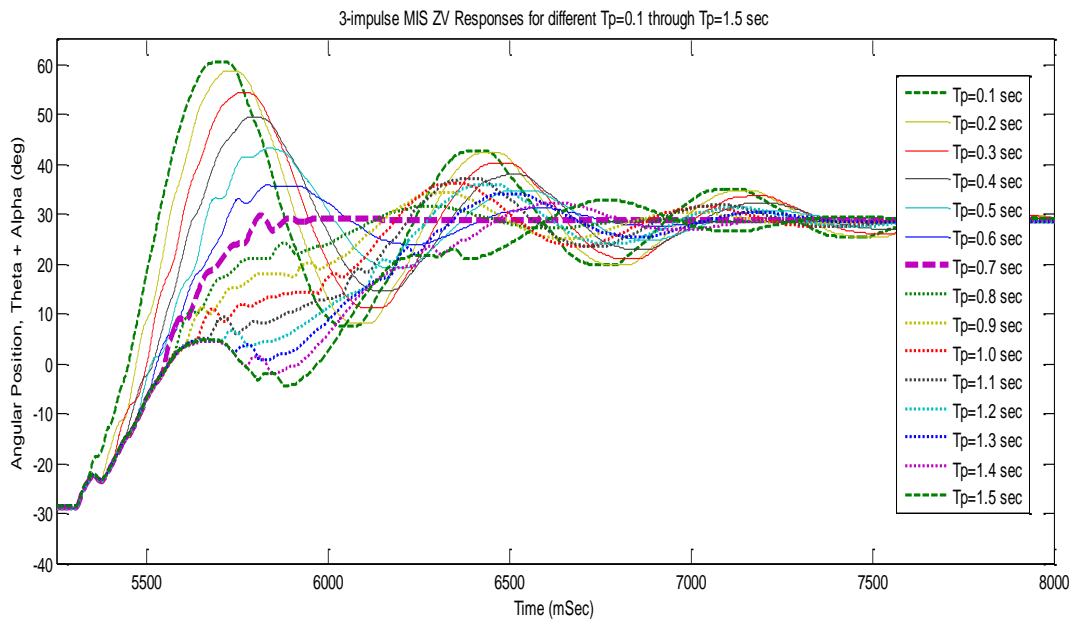


**Figure 12: 3-impulse MIS ZV Resp. – Experimental**

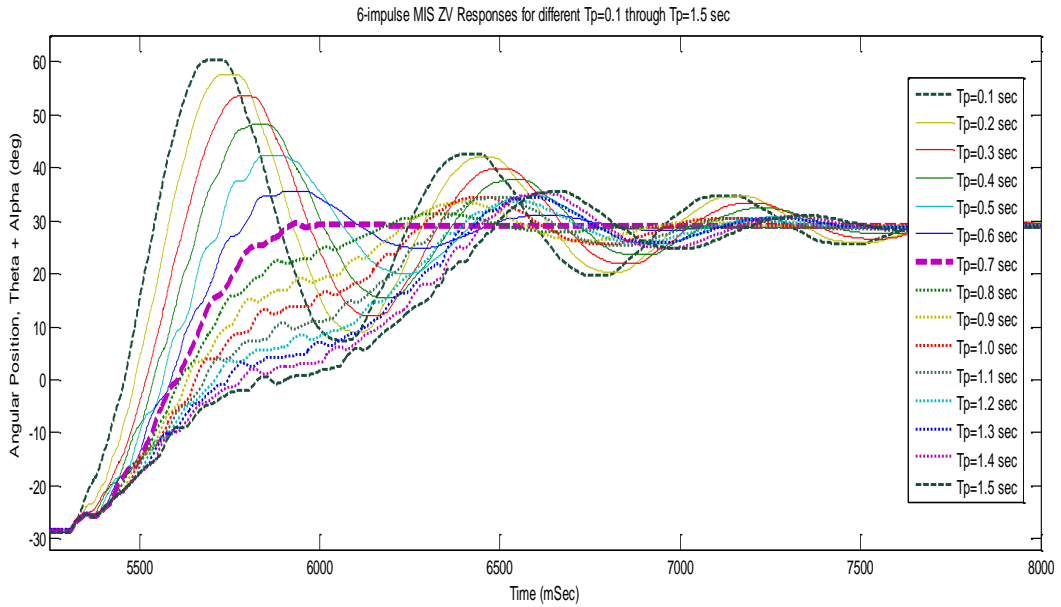


**Figure 13: 6-impulse MIS ZV Resp. – Experimental**

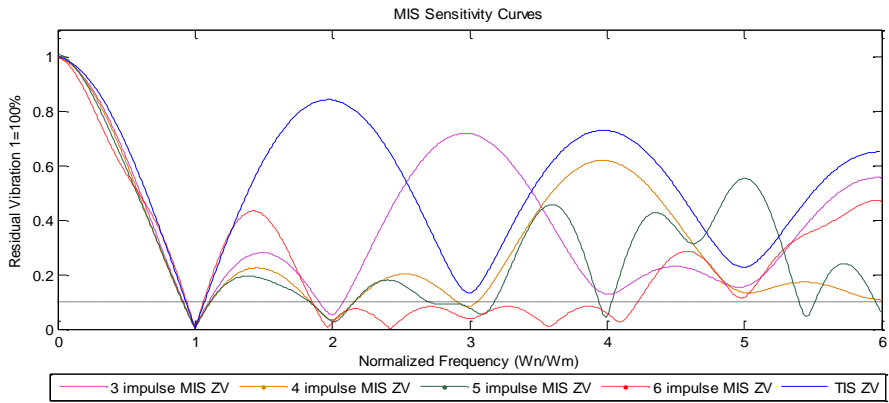


**Figure 14: MIS ZV shapers sensitivity curves – wider range – Simulation**

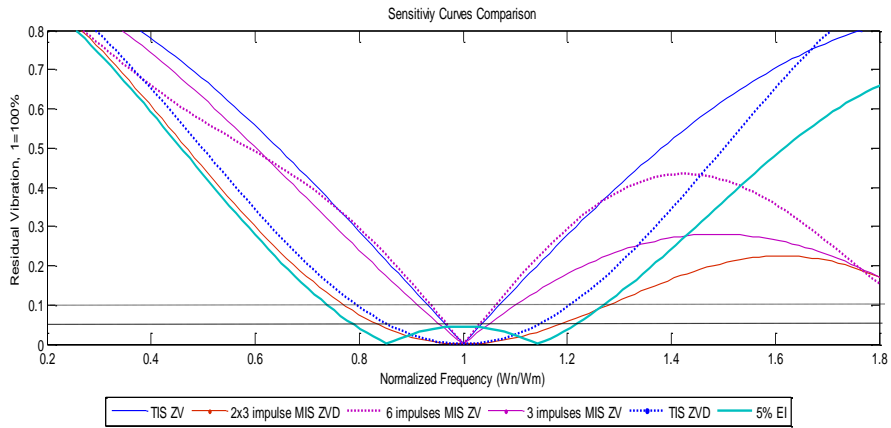


**Figure 15: TIS, MIS, EI sensitivity curves comparison – Simulation**

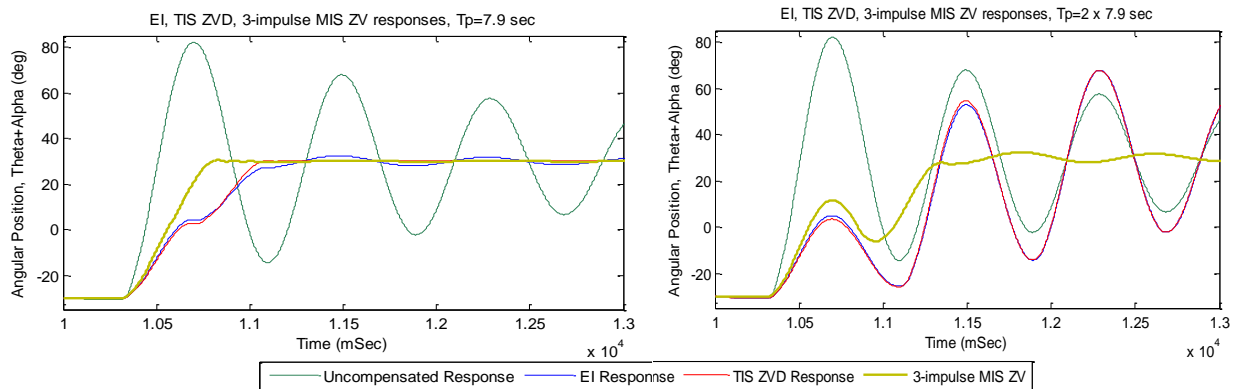


**Figure 16:  $\theta + \alpha$  3-Impulse MIS ZV, EI, and TIS ZVD Responses – Experimental**

### **ACKNOWLEDGMENTS:**

This work is supported by the national ANR-JCJC C-MUMS-project (National young investigator project ANR-12-JS03007.01: Control of Multivariable Piezoelectric Microsystems with Minimization of Sensors). This work is also supported by the LABEX ACTION.

### **REFERENCES:**

- [1] O.J.M. Smith, Posicast Control of Damped Oscillatory Systems, *Proceedings of the IRE*, 1957, pp.1249-1255
- [2] M. J. Robertson and W. E. Singhose, Closed-Form Deflection-Limiting Commands, *American Control Conference*, Portland, USA, 2005, pp.2104-2109
- [3] N.C. Singer and W.P. Seering, Preshaping Command Inputs to Reduce System Vibration, *Journal of Dynamic Systems, Measurement and Control*, 112, 1990, pp.76-82
- [4] W. Singhose, E. Crain and W. Seering, Convolved and Simultaneous Two-Mode Input Shapers, *IEE Proc. Control Theory Appl.*, Vol. 144, No. 6, 1997, pp.515-520
- [5] W. Singhose and N. Singer, Effects of Input Shaping on Two-Dimensional Trajectory Following, *IEEE Trans. on Robotics and Automation*, Vol. 12, No. 6, 1996, pp.881-887
- [6] T. Chang, K. Godbole and E. Hou, Optimal Input Shaper Design for High-Speed Robotic Workcells, *J. Vibration and Control*, Vol. 9, 2003, pp.1359-1376
- [7] C. F. Cutforth and L. Y. Pao, Control Using Equal Length Shaped Commands to Reduce Vibration, *IEEE Trans. on Control Sys. Tech.*, Vol. 11, No. 1, 2003, pp.62-72
- [8] Tuttle, T.D. and Seering, W.P., 1994, "A zero-placement technique for designing shaped inputs to suppress multiple mode vibration," in Proceedings of the American Control Conference, Baltimore, MD, pp. 2533-2537
- [9] Singhose, W.E. and Mills, IV.W., 1999, "Command generation using specified-negative amplitude input shapers," in Proceedings of the American Control Conference, San Diego, CA, pp. 61-65

- [10] Park, IV.J., Lee, J.W., Lim, IV.D., and Sung, Y.G., 2001, "Design and sensitivity analysis of an input shaping filter in the z-plane," *Journal of Sound and Vibration* 243, 157–171
- [11] J. Shan, H.-T. Liu, D. Sun, Modified input shaping for a rotating single-link flexible manipulator, *Journal of Sound and Vibration* 285 (1–2) (2005) 187–207
- [12] Gürleyük S.S., Optimal Unity-Magnitude Input Shaper Duration Analysis, *Archive of Applied Mechanics*, Vol.77, No.1, 2007, pp.63-71.
- [13] Gürleyük S.S., Hacıoğlu R. ve Cinal Ş., Three-Step Input Shaper for Damping Tubular Step Motor Vibrations, *J. of Mechanical Engineering Science*, Vol. 221, No.1, 2007, pp.1-9.
- [14] W. Singhose, W. Seering, N. Singer, Residual vibration reduction using vector diagrams to generate shaped inputs, *Journal of Mechanical Design* 116 (2) (1994) 654–659.
- [15] W.E. Singhose, L.J. Porter, T.D. Tuttle, N.C. Singer, Vibration reduction using multi-hump input shapers, *ASME Journal of Dynamic Systems Measurement and Control* 119 (2) (1997) 320–326.
- [16] QUANSER flexible link manual.
- [17] M. Rakotondrabe, 'Smart materials-based actuators at the micro/nano-scale: characterization, control and applications', edited book, Springer - Verlag, New York, ISBN 978-1-4614-6683-3, 2013
- [18] M. Rakotondrabe, 'Piezoelectric systems for precise and high dynamic positioning: design, modeling, estimation and control', HDR habilitation thesis, University of Franche-Comté / FEMTO-ST, November 10, 2014.
- [19] M. Rakotondrabe, C. Clévy and P. Lutz, 'Complete open loop control of hysteretic, creeped and oscillating piezoelectric cantilever', *IEEE - Transactions on Automation Science and Engineering (T-ASE)*, Vol.7(3), pp:440-450, July 2010.
- [20] M. Rakotondrabe, C. Clévy and P. Lutz, 'Hysteresis and vibration compensation in a nonlinear unimorph piezocantilever', *IEEE/RSJ - IROS*, (International Conference on Intelligent Robots and Systems), pp:558-563, Nice France, Sept 2008.
- [21] Y. Al Hamidi and M. Rakotondrabe, 'Multi-Mode Vibration Suppression in 2-DOF Piezoelectric Systems Using Zero Placement Input Shaping Technique', *SPIE - Sensing Technology+Applications; Sensors for Next Generation Robots conference* , 9494-27, Baltimore Maryland USA, April 2015.
- [22] M. Rakotondrabe, K. Rabenoroso, J. Agnus and N. Chaillet, 'Robust feedforward-feedback control of a nonlinear and oscillating 2-dof piezocantilever', *IEEE - Transactions on Automation Science and Engineering (T-ASE)*, Vol.8, Issue.3, pp.506-519, July 2011.
- [23] D. Habineza, M. Rakotondrabe and Y. Le Gorrec, ' Simultaneous Suppression of Badly-Damped Vibrations and Cross-couplings in a 2-DoF piezoelectric actuator, by using Feedforward Standard H-inf approach', *SPIE - Sensing Technology+Applications; Sensors for Next Generation Robots conference* , 9494-29, Baltimore Maryland USA, April 2015.